PMM U.S.S.R., Vol. 46, No. 5, pp. 621-625, 1983.
Printed in Great Britain.

0021-8928/83 $7.50+0.00

UDC 534.222.2

SUPERSONIC FLOW OVER A THIN WEDGE INTERSECTED BY THE FRONT OF AN EXTERNAL PLANE COMPRESSION SHOCK*

L.E. PEKUROVSKII

The steady-state three-dimensional self-similar problem of supersonic flow of perfect gas over a thin wedge is considered in the case when the flow is intersected by the front of an external plane compression shock normal to the wedge plane of symmetry. Geometric parameters (in particular the angle between the wedge edge and the front plane are selected so as to make this problem suitable for use as a scheme for simulating the flow in which an external shock generated by the fuselage interacts with a wedge representing the thin wing of an aircraft. Such interaction of an external compression shock with the weak shock produced by the wedge is in the majority of cases irregular. Pressure distribution on the wedge surface and over the external shock front is defined by elementary functions, and the pressure over the wedge is determined. Conditions under which the line of intersection of shocks can be in close proximity to the wedge, with pressure over the wedge behind the external compression shock changing abruptly, are indicated.

1. The pattern of flow. Let a uniform supersonic stream pass through the front of a plane compression shock, with the stream velocity vector at some angle to the front plane. Let us consider the small perturbation of that flow induced by a thin flat wedge which is stationary relative to the front which intersects the wedge so that part of its edge is in the unperturbed stream of gas, while the other part is in the gas stream that has passed through the compression shock from (Fig.1). The velocity vector of gas particles that have not yet passed through the shock front is, as usual, assumed to lie in the wedge plane of symmetry which is moreover normal to the plane of that shock front.

Gas particles that have passed through the compression shock front at the point of its intersection with the edge (surface a and point O, respectively in Fig.1). All notation in this Section conforms to that in Fig.1 become in their further motion sources of small perturbations propagating at supersonic velocity through the gas behind the shock. These perturbations are concentrated in the region bounded by the wall, the distorted part $OIGF$ of the shock front and by the Mach cone (surface b) whose vertex is at point O and axis OE directed along the velocity vector of gas behind the shock. Adjacent to that region is region 5 of constant perturbations, bounded by the weak compression shock front surface c attached to that part of the edge over which flows the supersonic stream of gas that has passed through the compression shock (region 1). This front is either tangent to the Mach cone, as shown in Fig.1, or intersects the compression shock front along some line lying above OI. In the second case the interaction of shocks results in the appearance of a reflected shock which is tangent to the Mach cone surface. In the gas stream ahead of the compression shock, perturbations induced by the wedge are constant; their region is bounded by the wall, the weak oblique compression shock attached to the edge attached to the edge by surface d, and part OGF of the compression shock front surface (region 2 on Fig.1).

Depending on parameters values that define the flow, line OG of front intersection may lie either outside the limits of the perturbed part of the compression shock front or belong to it. In the first case the interaction of waves is regular, with a further region of perturbed uniform stream formed behind the shock. That region is bounded by the weak diffracted shock tangent to the Mach cone, a part of the latter, and the compression shock front. In the second case, shown in Fig.1, the interaction of waves is irregular. In the reference system attached to the interaction line of fronts and moving along it so that velocity vectors of gas particles entering the fronts of interacting waves are normal to the intersection line, and since the gas velocity behind the shock wave is subsonic, no diffraction pressure shock can exist behind the shock wave. The straight line OG, thus, represents the line of intersection of only three compression shocks, one of which is weak. From the intersection line

*Prikl.Matem.Mekhan.,46,No.5,pp.777-783,1982

also issues the contact discontinuity surface that separates the gas particles which have passed through the front of the weak oblique shock and part of the external shock front, from particles which have passed through the external shock front only (the contact discontinuity surface is not shown in Fig.1).

Shock wave diffraction on a thin wedge in a sliding motion relative to the wave front was studied in /1/ in the case of irregular interaction of the incident wave and the compression shock induced by the wedge. A similar problem but in the case of regular interaction was analyzed in /2/. The flow pattern, i.e. the relative position of compression shocks, their orientation with respect to stream velocity vectors, position of the wall, etc., in these diffraction problems is similar to that described above (the stationary external shock wave relative to the wedge corresponds here to the incident shock wave).

It is expedient to select as input parameters of the problem those that would enable us to consider the flow defined above as the model of flow around some aircraft with the compression shock induced by the fuselage intersecting the compression shock produced by the wing (wedge). The fuselage is assumed to be a cone, more exactly, the angle the oncoming stream velocity vector and the external compression shock front plane is assumed to be equal the apex half-angle of the conical shock generated by the flow over the cone of a given apex angle, whose axis coincides with the direction of the oncoming stream velocity vector.

As the input parameters we select: the Mach number M_0 of the unperturbed oncoming stream, the angle χ in the symmetry plane of the wedge/wing between the normal to the stream velocity vector and the wedge edge (the edge angle of sweep) and the half-angle ω of the fuselage cone apex. The half-angle ε of the wedge which represents the wing is taken as the small parameter of the problem.

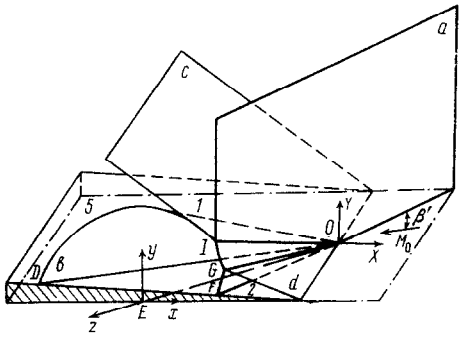

Fig.1

Besides these input parameters we have to consider also those whose relation to the determining parameters of the problem of shock wave diffraction by a thin wedge /1,2/ is the simplest, in order to establish the required correspondence between problems, and then use the data of /1,2/ for determining pressure perturbations in the stream behind the compression shock. Such parameters are: M_0, χ and β' which is the angle between the oncoming stream velocity vector and the plane of the unperturbed compression shock front (Fig.1). The dependence of angle β' on the input parameters ω and M_0 is given in /3,4/.

The relation between the indicated parameters and the input parameters is defined as follows:

$$M = M_0 \sin \beta', \quad M_\infty = M_0 \cos \chi, \quad \beta = \beta' + \chi + 90^\circ \tag{1.1}$$

where M and M_∞ are the Mach numbers of shock wave and wedge motion in the quiescent gas, respectively, and β is the angle of slip defined as the angle between the part of the shock wave front above the wedge surface and that part of the edge over which the front has already passed.

2. **Limits of regularity.** Taking into account formulas (1.1) and conditions $\beta > 90^\circ$, $\chi > 0$, we can obtain the equations of curves in the parameter plane χ, M_0 for fixed values of parameter β' which correspond to the regularity limits /1/

$$\chi = \operatorname{arctg} \frac{M_0 - R \sin \beta'}{R \cos \beta'} \tag{2.1}$$

$$R = \frac{M + c\,(M^2 + c^2 - 1)^{1/2}}{1 - c^2}, \quad c = \frac{a_1}{a_\infty} \sqrt{1 - m^2}, \quad M = M_0 \sin \beta'$$

$$\frac{a_1}{a_\infty} = \frac{[(\varkappa - 1) M^2 + 2]^{1/2} [2\varkappa M^2 - (\varkappa - 1)]^{1/2}}{(\varkappa + 1) M}, \quad m = \left[\frac{(\varkappa - 1) M^2 + 2}{2\varkappa M^2 - (\varkappa - 1)} \right]^{1/2}$$

where $\varkappa$ is the adiabatic exponent. These curves are shown in Fig.2 by dash lines for $\varkappa = 1.4$ and the indicated there values of β'. The domain of possible values of these parameters is upper bounded by the solid line curve whose equation is of the form

$$\chi = 90^\circ - \arcsin (1/M_0)$$

which follows from the conditions $\chi \leqslant 90^\circ - \beta'$, $\beta' > \arcsin(1/M_0)$.

Regular interactions correspond to the regions lying to the left of these lines.

Using formula (2.1) and, for instance, tables in /3/ for the dependence of β' on M_0 and ω, it is possible to obtain the picture of regularity boundaries of the problem input parameters.

Curves determined in this way are shown by solid lines in Fig.2, where their corresponding half-angles of the cone/fuselage apex are also indicated. The upper curve which corresponds to the cone zero angle is the same as the previously mentioned upper bound of the region of possible values of χ, and for any M_0 and χ the shock interaction is regular. For the remaining values of the cone half-angle irregular interactions correspond regions above the indicated boundaries. When the cone half-angle exceeds 25°, the shock interaction is irregular for any M_0 and χ.

If follows from Fig.2 that for any selection of the sweep-back angle of the wing edge and of the cone/fuselage aperture angle, change of type the interaction of shocks may occur twice as M_0 increases: first, for fairly low M_0 there is transition from the irregular to the regular type, followed by transition back again to the irregular type with further incrases of M_0. Hence if on practical consideration the analysis is limited to fairly large aperture angles of the cone/fuselage, the range of parameters for which the shock interaction is irregular, will appear explicitly predominate.

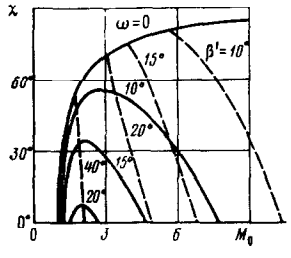

Fig.2

3. Pressure distribution over the wedge surface.

We introduce the orthogonal system of physical coordinates X, Y, Z whose origin is at point O (Fig.1), the Z axis coincides with the projection of the gas velocity vector behind the compression shock in the plane normal to the plane of the unperturbed shock front, and the Y axis normal to the Z axis in the front plane.

The considered here flow is conical. Its analysis is carried out in the plane normal to the Z axis. The dimensionless self-similar coordinates and dimensionless perturbations of pressure p are defined by formulas

$$x = \frac{X}{Z \operatorname{tg}\alpha}, \quad y = \frac{Y}{Z \operatorname{tg}\alpha}, \quad p = \frac{\tilde{p} - p_1}{\varepsilon \rho_1 a_1^2}$$

$$\left(\alpha = \arcsin\frac{\sin\mu}{m}, \quad \mu = \operatorname{arctg}\left[\frac{a_1}{a_\infty}\frac{m}{M_0}\frac{1}{\cos\beta'\cos(\beta'+\chi)}\right]\right)$$

where α is the Mach cone angle of the flow behind the compression shock, $\tilde{p}$ and p_1, are the dimensional values of pressure in the perturbed region (inside the Mach cone) and in region 1, respectively, and ρ_1 and a_1 are the dimensional values of density and speed of sound, respectively, in region 1.

The pressure perturbation in the gas behind the shock wave was obtained in /1/ in linear approximation with respect to ε. After the substitution in respective formulas (using formulas (1.1)) of M_0, χ, β' for M, M_∞, β, we obtain for the sought distribution of pressure perturbation the following formulas:

on the wedge surface (where p_5 is the perturbed pressure in region 5)

$$p[\tau(x)] = p_5 - \sum_{i=1}^{4} c_i \operatorname{arctg}\left(\frac{\gamma_i - \sqrt{2}}{\gamma_i + \sqrt{2}}\right)^{1/2}\tau - c_5 \operatorname{arctg}\frac{2y_G^*\tau}{1-\tau^2} + c_0 \ln\frac{\tau^2 - 2(1-y_G^{*2})^{1/2}\tau + 1}{\tau^2 + 2(1-y_G^{*2})^{1/2}\tau + 1} \qquad (3.1)$$

$$\tau = [(1-x_0)(1+x)/(1+x_0)(1-x)]^{1/2}$$

and along the pressure shock front

$$p(y) = -\frac{1}{2}\sum_{i=1}^{3} d_i \operatorname{arctg}\left[\frac{(\gamma_i^2-2)(y_0^2-y^2)}{2y_0^2}\right]^{1/2} - c_0 \ln\frac{[(y_0^2-y_G^2)^{1/2} + (y_0^2-y^2)^{1/2}]^2}{|y_G^2 - y^2|} - \frac{S}{b^2+1}\vartheta(y_G - y) \qquad (3.2)$$

where

$$p_5 = \frac{M_1\cos\beta + (a_\infty/a_1)M_0\cos\chi}{\{[M_1\cos\beta + (a_\infty/a_1)M_0\cos\chi]^2 - 1\}^{1/2}}$$

$$M_1 = \frac{2}{\varkappa+1}M_0\sin\beta'\frac{a_\infty}{a_1}\left(1 - \frac{1}{M_0^2\sin^2\beta'}\right)$$

$$y_0 = (1 - x_0^2)^{1/2}, \quad x_0 = m\cos\alpha/\cos\mu$$

$$c_{1,2} = \frac{4\gamma_{1,2}}{\pi(\gamma_{1,2}^2 - 2)^{1/2}} \frac{\gamma_1 + \gamma_2}{\gamma_{2,1} - \gamma_{1,2}} \left[\frac{(\gamma_3^2 - 2)^{1/2}}{\gamma_3 - \gamma_{1,2}} p_5 + \right.$$
$$\left. s(Ay_0^2 - x_0 B) y_G^* + \frac{y_0 \gamma_{2,1} K_0}{(\gamma_1 + \gamma_2) B} \right]$$

$$c_3 = \frac{2p_5}{\pi} \frac{(\gamma_1 + \gamma_3)(\gamma_2 + \gamma_3)}{(\gamma_1 - \gamma_3)(\gamma_2 - \gamma_3)}, \quad c_4 = \frac{2p_5}{\pi}, \quad c_5 = \frac{2}{\pi} \frac{S}{b^2 + 1}$$

$$c_6 = \frac{s}{\pi} y_G (y_0^2 - y_G^2)^{1/2}, \quad y_G^* = \frac{y_G}{y_0}, \quad s = \frac{y_G (y_0 h_u - m h_v)}{A y_G^2 - mB} - h_p$$

$$h_u = \frac{2}{\varkappa + 1} \frac{\cos\mu}{\cos\alpha} \frac{a_\infty}{a_1} \left\{ M_0 \sin\beta' \left[\frac{\varkappa + 1}{2} \frac{\sin(\beta' + \chi - \mu)}{\cos\mu} - \right.\right.$$
$$\left.\left. \sin(\beta' + \chi) \right] - \frac{\cos\chi}{M_0 \sin^2\beta'} - \frac{\varkappa - 1}{2} \frac{M_0 \cos^2\chi}{\sin^2\beta'} \right\} \frac{1}{(M_0^2 \cos^2\chi - 1)^{1/2}},$$

$$h_v = \frac{a_\infty}{a_1} \frac{M_0 \cos\chi}{\cos\alpha}$$

$$h_p = \frac{4}{\varkappa + 1} \frac{p_\infty}{p_1} \left[\left(\frac{M_0^2}{2} \sin^2\beta' - \frac{\varkappa - 1}{4} \right) \cos\chi - \right.$$
$$\left. \sin\beta' \sin(\beta' + \chi) \right] \frac{M_0^2 \cos\chi}{(M_0^2 \cos^2\chi - 1)^{1/2}}$$

$$\frac{p_1}{p_\infty} = \frac{2\varkappa}{\varkappa + 1} M_0^2 \sin^2\beta' - \frac{\varkappa - 1}{\varkappa + 1}, \quad \vartheta(y_G - y) = \begin{cases} 0, & y > y_G \\ 1, & y < y_G \end{cases}$$

$$A = \frac{M_0^2 \sin^2\beta' \cos(\beta' + \mu) + \cos(\beta' - \mu)}{2M_0^2 \sin^2\beta' \cos\alpha \cos\beta'} \left[\frac{2\varkappa M_0^2 \sin^2\beta' - (\varkappa - 1)}{2 + (\varkappa - 1) M_0^2 \sin^2\beta'} \right]^{1/2}$$

$$B = \frac{\varkappa + 1}{2} \frac{M_0^2 \sin^2\beta' - 1}{2 + (\varkappa - 1) M_0^2 \sin^2\beta'} \frac{1}{\cos^2\mu}$$

$$\gamma_{1,2} = \sqrt{2} x_0 M_0 \sin\beta' \{ M_0 \sin\beta' \pm (M_0^2 \sin^2\beta' - 1) \times$$
$$[M_0^2 \sin^2\beta' + 2/(\varkappa - 1)]^{-1/2} \}$$

$$\gamma_3 = \left[1 + \frac{(1 - x_0 x_1)^2 + y_0^2 y_1^2}{(1 - x_0 x_1)^2 - y_0^2 y_1^2} \right]^{1/2}, \quad \gamma_4 = -\gamma_3$$

$$x_1 = \frac{\sin(\beta' + \chi - \mu)}{\cos\alpha [M_\infty a_\infty / a_1 - M_1 \sin(\beta' + \chi)]}, \quad y_1 = (1 - x_1^2)^{1/2}$$

$$b = \frac{-y_G (y_0^2 - y_G^2)^{1/2}}{A y_G^2 - x_0 B}, \quad s = \frac{S}{(b^2 + 1)(A y_G^2 - x_0 B)}$$

$$d_1 = c_1, \quad d_2 = c_2, \quad d_3 = c_3 - c_4$$

$$K_0 = -\frac{b}{y_G} \left(h_p - \frac{S}{b^2 + 1} \right) - M_1 \sin(\beta' + \chi) \sec\alpha$$

In the xy plane in which the analysis is carried out, the distance between the triple point G of intersections of fronts to the wedge is defined by the formula

$$y_G = \frac{a_\infty}{a_1} \frac{M_0 \cos\beta' \cos(\beta' + \chi)}{(M_0^2 \cos^2\chi - 1)^{1/2}} \frac{\cos\alpha}{\cos^2\mu}$$

The inequalities $y_G < y_0$ $(y_G > y_0)$ correspond to irregular (regular) interactions.

Remarks. 1°. Formulas (3.1) and (3.2) are based on the assumption that $\gamma_1, \gamma_2 > \sqrt{2}$. Otherwise, for instance, when $\gamma_2 < \sqrt{2}$, it is necessary to substitute in the terms of formulas (3.1) and (3.2) with coefficients c_2 and d_2 the symbol Arth for arctg, and $2 - \gamma_2^2$ for $\gamma_2^2 - 2$ and $\sqrt{2} - \gamma_2$ for $\gamma_2 - \sqrt{2}$. The case of $\gamma_1 < \sqrt{2}$ is dealt similarly.

2°. If, as already mentioned in Sect.1, the weak compression shock generated by the wedge, which bounds region 5 in Fig.2, does not touch the Mach cone surface but intersects the external shock front, it is necessary to substitute in formula (3.1) and in coefficients c_3 and c_4 the remainder $p_5 - p_6$, for p_5, and add to the right-hand side of formula (3.2) p_6 which represents the pressure perturbation in the region originated by the reflection of the weak shock from the arbitrarily strong shock front; it can be determined using the reflection coefficient obtained in /5/.

Pressure perturbation along the shock front proved to be an abruptly varying function in the neighborhood of the intersection line of that front with the front of the weak oblique compression shock, where it has a composite singularity consisting of a discontinuity and logarithmic singularity. Because of this, when line OG is fairly close to the wall, a noticeable redistribution of pressure on the wall, as compared with the cases of regular shock interaction, is possible.

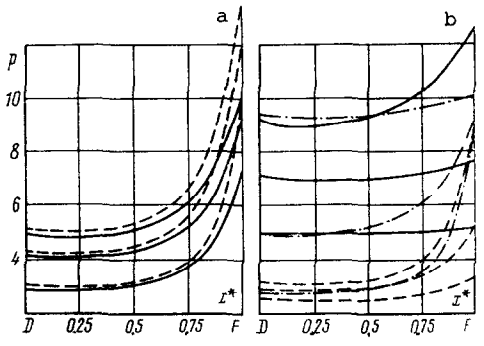

Fig.3

4. Calculation results. The formulas derived in Sect.3 and the indicated there tables enable us to obtain the distribution of pressure perturbation on the wedge surface for given input parameters M_0, χ, and ω.

Curves of pressure perturbation on the wedge are represented in terms of the coordinate $x^* = (1 - x)/(1 + x_0)$, where x_0 is the coordinate of point F of intersection of the compression shock front with the wall (the wedge), with $x^* = 0$ corresponding to point D and $x^* = 1$ to point F.

In the cases of irregular interaction of shock waves we used for computation the formula (3.1), and in that of regular interaction formulas of /2/ corrected in conformity with Sect.2 of /1/ were used. The adiabatic exponent was assumed equal (1.4).

The effect of the edge obliquity angle χ on pressure distribution on the wall for $\omega = 20°$ and $M_0 = 15$ is shown in Fig.3,a by solid lines and for $M_0 = 20$ by dash lines. The curves relate to angle χ equal 0, 20 and 40°. With increasing χ these curves lie one under the other.

As the edge obliquity angle is increased, an increase of the pressure gradient on the wall becomes noticeable near the compression shock front. This increase of pressure gradient takes place on the background of pressure perturbation decrease at each point, and is due to that the straight line OG approaches the wall as angle χ is increased. Since in the considered here cases the shock interaction is irregular, an abrupt change of pressure perturbation affecting its distribution takes place in the neighborhood of that straight line. For $M_0 = 15$, respectively $M_0 = 20$ we have $y_G^* = 0.343$ (0.265) in the case of $\chi = 0$ and $y_G^* = 0.225$ (0.175) and when $\chi = 40°$. In these formulas $y_G^* = y_G/y_0$, and y_0 and y_G are the coordinates of point I and G on the compression shock front. The comparison of solid lines ($M_0 = 15$) and dash lines ($M_0 = 20$) shows, moreover, that for each χ the higher pressure gradient corresponds to higher M_0.

The dependence of pressure distribution on M_0 is demonstrated by calculations with fixed values of angles ω and χ, as shown in Fig.3,b. Solid lines relate to $\omega = \chi = 10°$ and the dash lines to $\omega = 20°$ and $\chi = 40°$. Both sets of curves correspond to M_0 equal 6, 14 and 18. As M_0 is increased, pressure perturbation increases at every point of the wall, i.e. the curves lie one above the other.

The lower solid line ($M_0 = 6$) corresponds to regular shock interaction, while all the others to irregular interaction. For the indicated values of M_0 the quantity y_G^* is equal, respectively, 1.110, 0.669 and 0.562 for solid lines, and 0.421, 0.239 and 0.192 for the dash lines.

The dependence of pressure distribution on angle ω at $M_0 = 15$ and $\chi = 30°$ is shown in Fig.3,b by dash-dot lines. Angle ω was varied between 5° and 25° in steps of 10°. As this angle is increased, the curves lie one under the other, to them correspond the following values of y_G^* (from top to bottom): 0.851, 0.386 and 0.178.

REFERENCES

1. PEKUROVSKII L.E., Shock wave diffraction on a thin wedge moving with a slip relative to the wave front with irregular shock interaction. PMM, Vol.44, No.2, 1980.
2. SMYRL J.L., The impact of a shock wave on a thin two-dimensional aerofoil moving at supersonic speed. J. Fluid Mech., Vol.15, pt.2, 1963.
3. Tables of flow over pointed cones of hypersonic inviscid stream of air. Tr. TsAGI, iss. 1086, 1967.
4. KOCHIN N.E., KIBEL' I.A. and ROZE N.V., Theoretical Hydrodynamics, Pt.2. Moscow, FIZMATGIZ, 1963.
5. CHERNYI G.G., Flow of Gas at High Supersonic Speed. Moscow, FIZMATGIZ, 1959. (See also, in English, Introduction to hypersonic flow. Academic Press, N.Y. & London, 1961).

Translated by J.J.D.